Hilbert Schmidt Independence Criterion based Sensitivity Analysis for Grid Forming Inverter Dynamic Model

Balaji Guddanti*, Rajarshi Roychowdhury†, Logan McCloud*, Mahesh S. Illindala‡, Xuan Wu§
**Grid Integration & Stability*, *General Electric Vernova*, Schenectady, USA
balaji.guddanti@gevernova.com, logan1.mccloud@gevernova.com
†*Transmission Planning*, *Xcel Energy*, Denver, USA
rajarashiroychowdhury@ieee.org
‡*Department of Electrical & Computer Engineering*, *The Ohio State University*, Columbus, USA
millindala@ieee.org
§*Transmission Planning & Interconnections*, *Pedernales Electric Cooperative*, Johnson City, TX, USA
xuan.wu@peci.com

***Abstract*—Western Electricity Coordinating Council (WECC) recently approved the first generation Grid Forming (GFM) inverter models, which are now available in PSLF and PSS®E. As the dynamic behavior of these models depends on a large number of parameters, systematic parameter identification approaches for model validation are essential to maintain accuracy in planning studies. This paper addresses this gap by systematically quantifying the influence of GFM model parameters on key dynamic response performance metrics at the Point of Interconnection (POI). The principal objective is to identify and rank the parameters of the WECC approved generic model (REGFM_A1) that most strongly impact voltage, reactive power, active power, and frequency dynamics. The methodology employs the Hilbert Schmidt Independence Criterion (HSIC) as a kernel-based global sensitivity analysis tool, applied to time-domain simulation data from PSS®E. Validation of the sensitive parameters is performed through elasticity analysis and perturbation studies on a single-machine infinite bus system and a 200-bus synthetic grid network. The findings conclude that HSIC-based analysis provides a robust, data-driven method to guide parameter prioritization, enabling more effective model validation and more reliable stability assessments in the inverter-dominated power system network.**

***Index Terms*—grid forming inverter, model validation, nonlinear dynamic model, sensitivity analysis, WECC**

I. Introduction

The transition toward inverter-dominated power systems has accelerated the adoption of Grid Forming (GFM) Inverter-based Resources (IBRs) [1]. Unlike grid-following controls, GFM inverters can establish voltage and frequency references, offering system benefits such as inertia emulation, black-start capability, and robust disturbance recovery [2]. These promising attributes are key enablers for accommodating higher levels of renewable energy penetration. Recognizing their importance, research initiatives led by institutions across North America have developed generic GFM IBRs models [3], [4], now implemented in positive-sequence simulation tools like PSLF and PSS®E. These latest models provide system operators and planners with the means to evaluate GFM dynamics in planning studies.

There has been significant recent research on the modeling and control of GFM IBRs. A detailed survey, critically reviewing different GFM control technologies, is presented in [5]. A data-driven modeling approach for GFM inverters, validated through hardware-in-the-loop experimentation, is given in [6]. In [7], positive-sequence modeling framework for droop-controlled grid-forming inverters is proposed which suitable for large-scale transient stability studies. Despite these advances, there remains limited guidance on how GFM IBRs model parameters influence dynamic performance metrics for the quantities at the Point of Interconnection (POI). In parallel, Independent System Operators have introduced strict model validation and acceptance requirements, such as the ERCOT Model Quality Test [8] and the PJM model requirements [9], underscoring the need for accurate and reliable inverter models. Therefore, understanding the sensitivity and influence of generic GFM IBRs dynamic model parameters on dynamic response metrics is critical for effective model validation, large-signal stability analysis, and robust transmission planning studies in inverter-dominated grids.

The gap between detailed model development and practical parameter guidance highlights the need for additional analysis methods. Sensitivity analysis addresses this by linking parameter variations to performance metrics and identifying critical parameters for validation and tuning. The role of sensitivity analysis in quantifying uncertainty and guiding robust power system studies is highlighted in [10]. Trajectory Sensitivity Analysis [11] has been widely used in power system studies [12], [13]; however, its inability to capture nonlinear effects restricts its suitability for nonlinear models, including GFM IBR models. This limitation is addressed by Global Sensitivity Analysis techniques, including Sobol and Morris, which have been successfully used to identify key parameters in grid-following IBR models [14], [15]. However,

979-8-3315-8138-1

a clear link between sensitive parameters and their impact on dynamic response performance metrics is still unexplored. Hilbert–Schmidt Independence Criterion (HSIC) [16] provides a powerful sensitivity analysis framework which be leveraged to quantify the dependence between GFM model parameters and dynamic performance metrics. Unlike variance-based approaches such as Sobol or screening methods like Morris, HSIC can capture nonlinear and non-monotonic dependencies, making it particularly well-suited for analyzing the nonlinear dynamics of GFM IBR models.

This work presents an analytical data-driven approach to quantify the impact of the GFM inverter's model parameters on the dynamic response performance metrics. Unlike existing approaches that often rely on engineering intuition or hit-and-trial parameter tuning, the proposed HSIC based sensitivity analysis provides a robust method to systematically identify the parameters that exert the greatest influence on the quantities at the POI. The novelty of the work lies in supporting accurate model validation for GFM IBRs. The study demonstrates that the sensitivity results obtained through HSIC are largely independent of the underlying network size or configuration. By conducting the validation on both the Single Machine Infinite Bus (SMIB) system and on a 200-bus synthetic transmission grid, the work shows that the sensitive parameters remain consistent across different grid sizes. To justify robustness, the HSIC based sensitive parameters are independently validated using absolute elasticity analysis based on 30% parameter perturbations. This provides strong evidence that the proposed approach captures intrinsic model properties of the GFM inverter rather than artifacts of a particular test system.

The HSIC-based sensitivity analysis for the GFM inverter dynamic model is presented in Section II. The results are presented in Section III. The validation of the parameters on two different transmission grids is given in Section IV. Finally, the conclusion, followed by the future work directions, is presented in Section V.

II. Methodology

Let the nonlinear dynamic model of the GFM inverter be parameterized by a vector of parameters

$$\boldsymbol{\theta} = [\theta_1, \theta_2, \dots, \theta_p]^\top, \tag{1}$$

where p denotes the total number of tunable model parameters. For global sensitivity analysis, m independent realizations of these parameters are generated according to their respective operating ranges or probability distributions, forming the parameter sample matrix $\boldsymbol{\Theta}$,

$$\boldsymbol{\Theta} = [\boldsymbol{\theta}^{(1)}, \boldsymbol{\theta}^{(2)}, \dots, \boldsymbol{\theta}^{(m)}]^\top. \tag{2}$$

For each sampled parameter set $\boldsymbol{\theta}^{(i)}$, time-domain simulations are conducted in PSS®E to obtain the dynamic trajectories of voltage (V_{POI}), reactive power (Q_{POI}), active power (P_{POI}), and frequency (F_{POI}) at the Point of Interconnection (POI). From each trajectory, a vector of r dynamic response performance metrics (as shown in Table I) is computed and represented as

TABLE I
Dynamic Response Performance Metrics Description

Performance Metric	Intepretation
Delay Time ($\mathrm{t_d}$)	Time to reach 50% of steady state value
Rise Time ($\mathrm{t_r}$)	Time to reach 90% of steady state value
Peak Time ($\mathrm{t_p}$)	Time to reach the first peak of the overshoot
Settling Time ($\mathrm{t_s}$)	Time required for the oscillation to reach within ±5% of the steady state value
Maximum Overshoot ($\mathrm{m_p}$)	Maximum deviation above steady state value
Ramp Rate (rr)	Rate of change per unit time
Rate of Change of Frquency (rocof)	Maximum instantaneous rate of change of system frequency
Frequency Nadir ($\mathrm{f_{nadir}}$)	Lowest frequency point

$$\mathbf{M} = [M_1, M_2, \dots, M_r]^\top. \tag{3}$$

The complete dataset $\mathcal{D}$, of simulation outcomes can thus be expressed as

$$\mathcal{D} = \{(\boldsymbol{\theta}^{(i)}, \mathbf{M}^{(i)})\}_{i=1}^{m}. \tag{4}$$

The sensitivity between a given model parameter θ_p and a performance metric M_r is quantified using the HSIC, which measures the statistical dependence between two random variables in reproducing kernel Hilbert spaces (RKHSs).

The HSIC between θ_p and M_r is defined as

$$\mathrm{HSIC}(\theta_p, M_r) = \frac{1}{(m-1)^2}\,\mathrm{Tr}(\tilde{\mathbf{K}}^{(p)}\tilde{\mathbf{L}}^{(r)}), \tag{5}$$

where $\mathrm{Tr}(\cdot)$ denotes the trace operator, and $\tilde{\mathbf{K}}^{(p)}$ and $\tilde{\mathbf{L}}^{(r)}$ are the centered kernel matrices corresponding to θ_p and M_r, respectively.

The centered matrices are computed as

$$\tilde{\mathbf{K}}^{(p)} = \mathbf{H}\mathbf{K}^{(p)}\mathbf{H}, \qquad \tilde{\mathbf{L}}^{(r)} = \mathbf{H}\mathbf{L}^{(r)}\mathbf{H}, \tag{6}$$

where the centering matrix $\mathbf{H}$ removes mean effects and is given by

$$\mathbf{H} = \mathbf{I}_m - \frac{1}{m}\mathbf{1}\mathbf{1}^\top, \tag{7}$$

with $\mathbf{I}_m$ denoting the $m \times m$ identity matrix and $\mathbf{1}$ a column vector of ones of length m.

The elements of the uncentered kernel matrices are obtained using the Gaussian Radial Basis Function (RBF) kernel:

$$K_{ab}^{(p)} = \exp\left[-\frac{(\theta_p^{(a)} - \theta_p^{(b)})^2}{2\sigma_p^2}\right] \text{for all} \quad a, b \in \{1, 2, \dots, m\} \tag{8}$$

$$L_{ab}^{(r)} = \exp\left[-\frac{(M_r^{(a)} - M_r^{(b)})^2}{2\sigma_r^2}\right] \text{for all} \quad a, b \in \{1, 2, \dots, m\} \tag{9}$$

The kernel bandwidths σ_p and σ_r are determined using the median heuristic to ensure appropriate scaling between parameters and metrics.

979-8-3315-8138-1

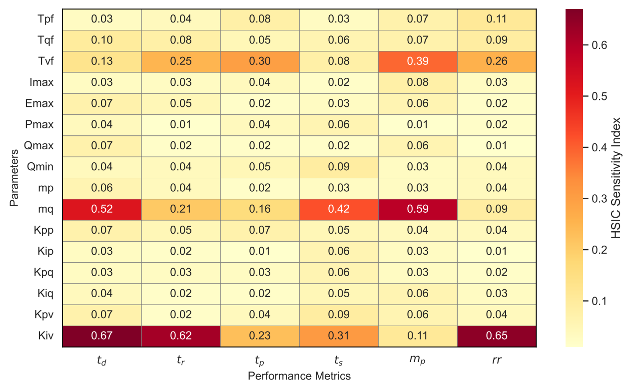

Fig. 1. Heatmap of REGFM_A1 HSIC Sensitivity Indices for $\mathrm{V_{POI}}$

To obtain a dimensionless and comparable measure of dependence, the HSIC value is normalized as

$$S_p^r = \frac{\mathrm{HSIC}(\theta_p, M_r)}{\sqrt{\mathrm{HSIC}(\theta_p, \theta_p)\,\mathrm{HSIC}(M_r, M_r)}}. \tag{10}$$

The normalized index $S_p^r \in [0,1]$ quantifies the degree of statistical dependence between the p-th parameter and the r-th performance metric. A higher S_p^r value indicates stronger nonlinear dependence and a greater influence of θ_p on M_r.

A multidimensional parameter space is constructed to span the practical range of variation for each model parameter based on engineering judgment and manufacturer specifications. Using Latin Hypercube Sampling (LHS) or equivalent low-discrepancy sequences, m parameter sets $\{\boldsymbol{\theta}^{(i)}\}_{i=1}^m$ are generated to ensure uniform coverage of the space.

For each parameter set, time-domain simulations are executed in PSS®E, and the corresponding dynamic performance metrics $\mathbf{M}^{(i)}$ are extracted following Table I. The resulting parameter–metric pairs $(\boldsymbol{\theta}^{(i)}, \mathbf{M}^{(i)})$ serve as inputs to the HSIC computation pipeline defined by (5)–(10). The sensitivity indices S_p^r are arranged in the sensitivity matrix

$$\mathbf{S} = \begin{bmatrix} S_1^1 & S_1^2 & \cdots & S_1^r \\ S_2^1 & S_2^2 & \cdots & S_2^r \\ \vdots & \vdots & \ddots & \vdots \\ S_p^1 & S_p^2 & \cdots & S_p^r \end{bmatrix}, \tag{11}$$

where each row corresponds to a model parameter and each column corresponds to a performance metric.

Parameters are ranked based on the magnitude of the normalized sensitivity indices S_p^r. Parameters exhibiting consistently high S_p^r values across performance metrics mentioned in Table I are identified as globally influential and prioritized for model validation and tuning. Visualization through heatmaps of the sensitivity matrix (11) provides an intuitive representation of parameter–metric dependencies, highlighting the dominant GFM control loops and dynamic parameters influencing voltage ($\mathrm{V_{POI}}$), reactive power ($\mathrm{Q_{POI}}$), frequency ($\mathrm{F_{POI}}$), and active power ($\mathrm{P_{POI}}$) at the POI.

III. Results

The proposed HSIC based sensitivity analysis presented in Section II is applied to the recently approved Western Electricity Coordinating Council [17] GFM inveter model, REGFM_A1. The objective of this analysis is to identify the GFM model parameters that have the strongest influence on the dynamic response performance metrics for $\mathrm{V_{POI}}$, $\mathrm{Q_{POI}}$, $\mathrm{F_{POI}}$, and $\mathrm{P_{POI}}$.

A total of $m = 500$ parameter sets were generated using LHS to uniformly explore the feasible parameter space defined for the REGFM_A1 model. For each parameter realization, time-domain simulations were performed in PSS®E to capture the inverter's dynamic response under a voltage and frequency step disturbance as recommended in [18]. Each simulation was carried out for 50 seconds, and the resulting time-series data for the quantities at the POI were post-processed to extract the dynamic response performance metrics defined in Table I. These metrics include $\mathrm{t_d}$, $\mathrm{t_r}$, $\mathrm{t_p}$, $\mathrm{t_s}$, $\mathrm{m_p}$, rr, along with rocof and $\mathrm{f_{nadir}}$ for the frequency step test.

The computed HSIC sensitivity indices for the parameters are shown in Figs. 1 − 4, corresponding to the dynamic performance of the quantities at the POI. In each heatmap, the horizontal axis represents the performance metrics mentioned in Table I, while the vertical axis lists the GFM inverter model parameters. Warmer colors indicate higher HSIC indices, signifying stronger dependence between a parameter and the selected performance metric. These visualizations provide a comprehensive mapping of parameter sensitivities, from which the most sensitive parameters ($S_p^r \geq 0.20$) are identified and summarized in Table II. Beyond visualization, the tabulated results highlight clear trends across both models. Parameters (mq, Tvf, Kiv, mp, Tpf, mp) directly associated with reactive and active power control loops consistently emerge with higher HSIC scores, confirming their dominant role in shaping voltage and frequency responses. Conversely, parameters tied to slower secondary dynamics show comparatively weaker influence, indicating their limited impact on the dynamic response performance metrics. This separation between sensitive and non-sensitive parameters provides practical guidance for

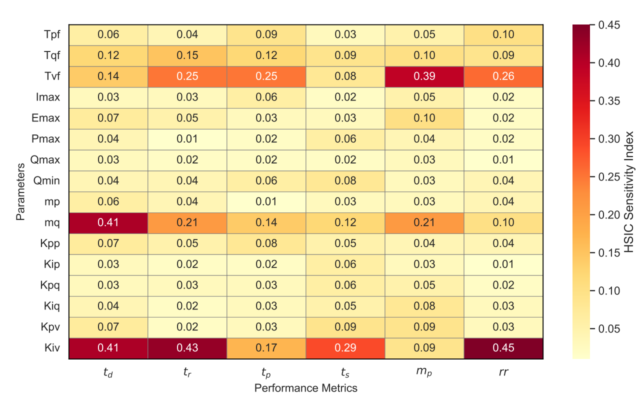

Fig. 2. Heatmap of REGFM_A1 HSIC Sensitivity Indices for $\mathrm{Q_{POI}}$

979-8-3315-8138-1

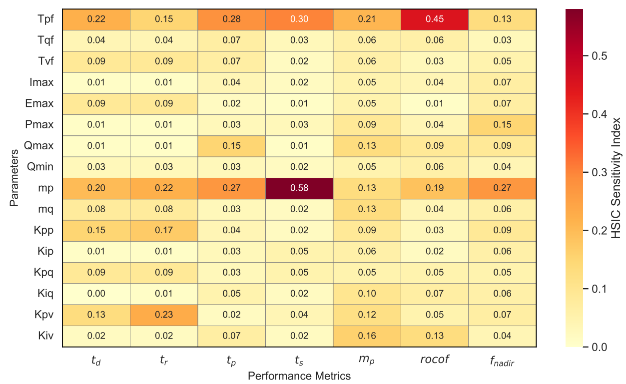

Fig. 3. Heatmap of REGFM_A1 HSIC Sensitivity Indices for F_{POI}

TABLE II
REGFM_A1 HSIC SENSITIVITY ANALYSIS RESULTS

Performance Metric	V_{POI}	Q_{POI}	F_{POI}	P_{POI}
t_d	mq, Kiv	mq, Kiv	mq, Kpv	mp, Kpv
t_r	Tvf, mq Kiv	Tvf, mq Kiv	mq, Kpv	Tpf, Pmax Kpv
t_p	Tvf, Kiv	Tvf	Tpf, mp	Tpf, mp
t_s	mq, Kiv	Kiv	Tpf, mp	Tpf, mp
m_p	Tvf, mq	Tvf, mq	Tpf	Tpf, mp Kip, Kiv
rr	Tvf, Kiv	Tvf, Kiv	–	Tpf, mp Kpp
rocof	–	–	Tpf	–
f_{nadir}	–	–	mp	–

model validation and parameter tuning, ensuring that the most critical parameters are prioritized during studies.

IV. Validation and Case Study

To validate the parameters identified by the HSIC based sensitivity analysis, we employ time-domain perturbation simulations in PSS®E. The central idea is to verify that parameters with high HSIC indices indeed exert a measurable influence on dynamic response performance metrics. A baseline simulation is first run with the nominal parameter set provided in [3]. Then, each parameter of interest is perturbed individually by 30% while all other parameters are held constant. For each perturbed case, the local elasticity is computed. The local elasticity of a performance metric, $\mathcal{M}_r$, with respect to parameter θ_p is given as follows.

$$\mathcal{E}_{p\to r} = \frac{\Delta\mathcal{M}_r/\mathcal{M}_r}{\Delta\theta_p/\theta_p} \tag{12}$$

In (12), $\Delta\mathcal{M}_r$ is the relative change in the metric due to perturbation of the parameter θ_p, and $\Delta\theta_p$ is the relative change applied to the parameter. A higher absolute elasticity value indicates that the parameter has a stronger influence on the metric. In addition to elasticity, the time-domain response trajectories under perturbed parameters are compared with the baseline to visually confirm the nature and magnitude of parameter effects. This validation procedure is performed on two different networks to test both isolation and scalability: a Single-Machine Infinite Bus (SMIB) case, and a 200-bus synthetic grid network.

A. SMIB

The first validation study is carried out using a SMIB system with a 100 MW GFM IBR modeled using the REGFM_A1 representation. This system provides a controlled environment in which the influence of individual parameters can be directly observed, free from the masking effects of network interactions.

Parameters identified as most sensitive by the HSIC-based screening (Table II) were perturbed by 30% relative to their nominal values, and the resulting dynamic responses were analyzed. For a voltage step at the POI, the parameters Tvf and Kiv exhibit the highest elasticities, with magnitudes of 0.97, 0.89, and 0.95 corresponding to t_d, t_r, and t_p, respectively. These high elasticity values confirm that even moderate variations in the fast voltage-control loop parameters significantly affect the transient voltage and reactive power response. A three-phase bolted fault at the POI, cleared within 10 cycles, is applied as the primary disturbance to evaluate the model's dynamic behavior. The corresponding

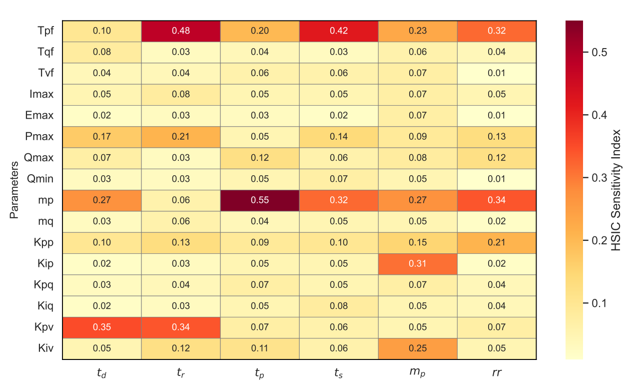

Fig. 4. Heatmap of REGFM_A1 HSIC Sensitivity Indices for P_{POI}

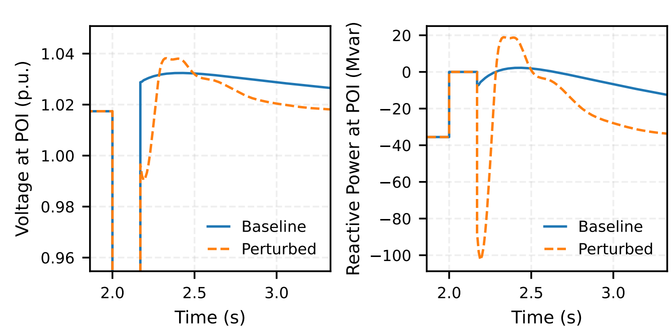

Fig. 5. Comparison of V_{POI} and Q_{POI} trajectories in the SMIB system with the 100 MW REGFM_A1 model under sensitive parameter perturbations

979-8-3315-8138-1

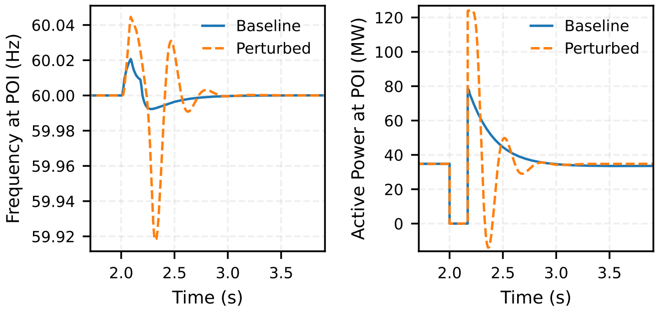

Fig. 6. Comparison of $\mathrm{F_{POI}}$ and $\mathrm{P_{POI}}$ trajectories in the 200-bus network with the 150 MW REGFM_A1 model under sensitive parameter perturbations

time-domain trajectories in Fig. 5 visually corroborate the quantitative results—perturbations in the sensitive parameters lead to pronounced deviations from the baseline.

B. 200-Bus Synthetic Grid Network

The second validation is conducted on a 200-bus synthetic grid with a 150 MW REGFM_A1. This large system captures network interactions and load diversity.

Parameters presented in Table II were perturbed by 30% relative to their nominal values, and the resulting dynamic responses were analyzed. For a frequency step at the POI, the parameters Tpf and mp exhibit the highest elasticities, with magnitudes of 0.91 and 0.97 corresponding to $\mathrm{t_r}$ and $\mathrm{m_p}$, respectively. These results indicate that the fast active-power control loop strongly governs frequency recovery and overshoot following a disturbance. A three-phase bolted fault at the POI (bus 152), cleared within 10 cycles, is simulated to evaluate the robustness of these sensitive parameters. The time-domain responses in Fig. 6 confirm the perturbations in Tpf and mp produce noticeable deviations in frequency and active power trajectories compared to the baseline case.

V. Conclusion

This paper introduces an HSIC based sensitivity analysis framework to quantify the dependence of GFM IBR model parameters on dynamic performance in power systems. The motivation stems from the fact that recently approved WECC GFM models, available in PSS®E and PSLF, include a large number of parameters that strongly shape their dynamic response, yet there is limited clear guidance for their tuning and validation. The research achieved two major outcomes. First, the methodology was developed to obtain the sensitive parameters affecting the dynamic response of the quantities at the POI. Second, the validation studies demonstrated that the HSIC-based rankings remain valid across different system scales and inverter sizes. In a SMIB configuration with a 100 MW REGFM_A1 GFM IBR elasticity analysis and time-domain trajectories confirmed the influence of POI quantities related parameters. Additionally, in a 200-bus synthetic grid with a 150 MW GFM IBR, the time-domain response for the POI quantities similarly validated the sensitivity results. The benefits of the proposed framework are clear. It replaces intuition and trial-and-error with a data-driven and analytical tool for identifying critical parameters, provides results that are network-independent, and directly supports model validation, parameter tuning, and planning studies. Future directions include extending the approach to multi-inverter systems, exploring mixed grid-forming and grid-following interactions.

References

[1] J. Matevosyan, B. Badrzadeh, T. Prevost, E. Quitmann, D. Ramasubramanian, H. Urdal, S. Achilles, J. MacDowell, S. H. Huang, V. Vital, J. O'Sullivan, and R. Quint, "Grid-forming inverters: Are they the key for high renewable penetration?" *IEEE Power and Energy Magazine*, vol. 17, no. 6, pp. 89–98, 2019.

[2] B. Bahrani, M. H. Ravanji, B. Kroposki, D. Ramasubramanian, X. Guillaud, T. Prevost, and N.-A. Cutululis, "Grid-forming inverter-based resource research landscape: Understanding the key assets for renewable-rich power systems," *IEEE Power and Energy Magazine*, vol. 22, no. 2, pp. 18–29, 2024.

[3] W. Du, R. H. Lasseter, C. Hardt *et al.*, "Model specification of droop-controlled, grid-forming inverters (regfm_a1)," PNNL, Tech. Rep. PNNL-35110, 2023.

[4] W. Du, S. Achilles, D. Ramasubramanian *et al.*, "Virtual synchronous machine grid-forming inverter model specification (regfm_b1)," UNIFI Consortium, Tech. Rep. UNIFI-2024-6-1, 2024.

[5] M. Tozak, S. Taskin, I. Sengor, and B. P. Hayes, "Modeling and control of grid forming converters: A systematic review," *IEEE Access*, vol. 12, pp. 107 818–107 843, 2024.

[6] N. Guruwacharya, S. Chakraborty, G. Saraswat, R. Bryce, T. M. Hansen, and R. Tonkoski, "Data-driven modeling of grid-forming inverter dynamics using power hardware-in-the-loop experimentation," *IEEE Access*, vol. 12, pp. 52 267–52 281, 2024.

[7] W. Du, Q. H. Nguyen, S. Wang, J. Kim, Y. Liu, S. Zhu, F. K. Tuffner, and Z. Huang, "Positive-sequence modeling of droop-controlled grid-forming inverters for transient stability simulation of transmission systems," *IEEE Transactions on Power Delivery*, vol. 39, no. 3, pp. 1736–1748, 2024.

[8] ERCOT, "Dynamics working group procedure manual," 2025, Revision 23.

[9] PJM, "PJM guidance for nerc mod-026-027 generation owner preparation and submittal," 2025.

[10] M. Ginocchi, F. Ponci, and A. Monti, "Sensitivity analysis and power systems: Can we bridge the gap? a review and a guide to getting started," *Energies*, vol. 14, no. 24, 2021. [Online]. Available: https://www.mdpi.com/1996-1073/14/24/8274

[11] I. Hiskens and M. Pai, "Trajectory sensitivity analysis of hybrid systems," *IEEE Transactions on Circuits and Systems I: Fundamental Theory and Applications*, vol. 47, no. 2, pp. 204–220, 2000.

[12] P. Mitra, V. Vittal, P. Pourbeik, and A. Gaikwad, "Load sensitivity studies in power systems with non-smooth load behavior," *IEEE Transactions on Power Systems*, vol. 32, no. 1, pp. 705–714, 2017.

[13] G. Hou and V. Vittal, "Determination of transient stability constrained interface real power flow limit using trajectory sensitivity approach," *IEEE Transactions on Power Systems*, vol. 28, no. 3, pp. 2156–2163, 2013.

[14] B. Guddanti, J. R. Orrego, R. Roychowdhury, and M. S. Illindala, "Sensitivity analysis based identification of key parameters in the dynamic model of a utility-scale solar pv plant," *IEEE Transactions on Power Systems*, vol. 37, no. 2, pp. 1340–1350, 2022.

[15] B. Guddanti, R. Roychowdhury, and M. S. Illindala, "Evaluation of modified global sensitivity analysis techniques for power system dynamic studies," in *2022 IEEE Industry Applications Society Annual Meeting (IAS)*, 2022, pp. 1–6.

[16] A. Gretton, O. Bousquet, A. Smola, and B. Schölkopf, "Measuring statistical dependence with hilbert-schmidt norms," in *Algorithmic Learning Theory*, S. Jain, H. U. Simon, and E. Tomita, Eds. Berlin, Heidelberg: Springer Berlin Heidelberg, 2005, pp. 63–77.

[17] Western Electricity Coordinating Council, "WECC approved dynamic model library," 2025, Version May.

[18] NERC, "Reliability guideline power plant model verification for invter-based resources," 2018.

979-8-3315-8138-1